Cost-effective Community Battery Sizing and Operation within a Local Market Framework

Nam Trong Dinh, *Student Member, IEEE,* Sahand Karimi-Arpanahi, *Student Member, IEEE,* S. Ali Pourmousavi, *Senior Member, IEEE,* Mingyu Guo, and Jon A. R. Liisberg

***Abstract*—Extreme peak power demand is a major factor behind high electricity prices, despite occurring only for a few hours annually. This peak demand drives the need for costly upgrades for the network asset, which is ultimately passed on to the end-users through higher electricity network tariffs. To alleviate this issue, we propose a solution for cost-effective peak demand reduction in a local neighbourhood using prosumer-centric flexibility and community battery storage (CBS). Accordingly, we present a CBS sizing framework for peak demand reduction considering receding horizon operation and a bilevel program in which a profit-making entity (leader) operates the CBS and dynamically sets mark-up prices. Through the dynamic mark-up and real-time wholesale market prices, the CBS operator can harness the demand-side flexibility provided by the load-shifting behaviour of the local prosumers (followers). To this end, we develop a realistic price-responsive model that adjusts prosumers' behaviour with respect to fluctuations of dynamic prices while considering prosumers' discomfort caused by load shifting. The simulation results based on real-world data show that adopting the proposed framework and the price-responsive model not only increases the CBS owner's profit but also reduces peak demand and prosumers' electricity bills by 38% and 24%, respectively.**

***Index Terms*—Peak demand, Community battery, battery sizing, bilevel optimisation, price-responsive model.**

NOMENCLATURE

Indices and Sets

n/N	Indices/Set of local prosumers
T	Set of time intervals in the sizing horizon
D^+, D^-	Convex hull of McCormick envelopes
H_j^{RB}	Set of time intervals in a rebound horizon
H_j	Set of time intervals in a receding horizon
i, k	Indices for Benders iterations
t, j, m	Indices for time intervals

Parameters

β	Prosumer price elasticity
$\overline{\lambda}^{\text{MU}}/\underline{\lambda}^{\text{MU}}$	Mark-up price upper/lower bound (\$/kWh)
$\hat{x}$	Prosumer original consumption (kWh)
$\overline{\text{SoC}}/\underline{\text{SoC}}$	Battery state-of-charge upper/lower bound (%)
$\alpha^{\text{up}}, \epsilon$	Parameters for Benders decomposition
Δt	Length of time interval (h)
Δx	Adjusted demand (kWh)
$\eta, R, \mathcal{T}$	Battery calendar loss parameters
Γ	Battery round-trip efficiency (%)
Λ	Prosumer's original payment (\$)
$\lambda^{\text{oNW}}/\lambda^{\text{pNW}}$	Operator/Prosumer network usage charge(\$/kWh)
λ^{peak}	Peak demand charge (\$/kW)
λ^{RT}	Real-time (RT) price (\$/kWh)
$\lambda^{\text{RT}}_{\text{min}}$	Lowest RT price in a receding horizon (\$/kWh)
λ^{sl}	Penalty coefficient for slack variable
$\overline{x}/\underline{x}$	Prosumer consumption upper/lower bound (kWh)
EoL	Battery end-of-life (%)
ExpL	Electricity export limit (kW)
a, b, c, κ, ξ	Battery cyclic loss parameters
B^{sup}	Network supply charge (\$)
$B_s, \Upsilon_s, \Theta_s$	Weighted sum of sub-problems results
E^{init}	Battery initial SoC (kWh)
E^{price}	Battery per-unit cost (\$/kWh)
G	Generated rooftop solar PV energy (kWh)
T^c	Minimum hours to fully charge the battery (h)
T^e	Battery expected lifetime (h)

Variables

x	Prosumer consumption (kWh)
α	Proxy of sub-problem objective function
λ^{MU}	Mark-up price (\$/kWh)
Υ, Θ	Dual variables for Benders decomposition
ζ	Peak demand threshold (kW)
B^{com}	Prosumers compensation cost (\$)
$B^{\text{cyc}}/B^{\text{cal}}$	Cost of battery cyclic/calendar degradation (\$)
$B^{\text{mas}}/B^{\text{sub}}$	Master/Sub-problem objective function
C	Prosumer comfort function
E	Energy level in battery (kWh)
E^{cap}	Battery capacity (kWh)
G^u/G^s	Used / Spilt solar energy (kWh)
n^+/n^-	Local market positive/negative net demand (kWh)
n^{sl}	Slack variable
P	Battery dispatch level (kW)
$P^{\text{ch}}/P^{\text{dis}}$	Battery charging/discharging power (kW)
P^{ope}	Operator profit (\$)
$Q^{\text{cal}}/Q^{\text{cyc}}$	Battery cyclic/calendar degradation (%)
U^{pro}	Prosumer utility
x^+/x^-	Prosumer positive/negative net demand (kWh)
z^+, z^-	Auxiliary variables for McCormick envelopes

I. INTRODUCTION

A. Motivation and literature review

THE rapid uptake of rooftop solar photovoltaic (PV) systems in recent years has made Australia the world leader in solar installation per capita. However, despite the oversupply during midday, solar energy is unavailable during the evening peak hours. This poses significant difficulties for distribution network service providers (DNSPs) (analogous to distribution system operators), who must frequently reinforce the networks to ensure system security and meet the high peak demand during early evening hours [1]. Then, such network upgrade expenses are passed on to network customers, e.g., as the peak demand tariff [2]. This peak demand charge, determined based on the maximum electricity consumption during a billing period, is typically imposed on commercial and industrial consumers as an incentive to flatten their consumption profiles. Due to the constant growth in residential

peak demand in recent years [3], many DNSPs in Australia have also mandated a peak demand tariff for new households connected to its distribution network [4]. Therefore, prosumers may still see their electricity bill increasing despite the high uptake of renewable energy sources.

One possible solution is to use residential batteries to shift excess rooftop PV generation to peak demand hours [5]. However, residential batteries are too expensive for most prosumers. Community battery storage (CBS) systems offer an attractive alternative, providing a lucrative middle ground solution to address the problem [6]. A fundamental benefit of using CBS is the management of peak power demand by taking advantage of excess rooftop PV generation during the day to meet peak hours in the evening [5]. The reduction in peak demand reduces the peak demand charge; hence, the electricity bill. However, this requires a CBS system with sufficient capacity to manage the maximum power below a peak demand threshold. Therefore, finding a trade-off between the maximum peak demand threshold and CBS capacity is essential to ensure cost-effective operation.

A growing number of studies have been published on the use of battery systems for peak demand reduction, from single-household level [7], [8] to large-scale buildings [9], [10]. In [7], the authors proposed a battery sizing model for peak load shaving by keeping demand below a predefined threshold. The authors in [8] formulated a multi-objective optimisation problem, aiming to minimise both the energy usage cost and the peak load with a focus only on the energy usage cost, not the peak demand charge. Similar work is reported in [9], where the authors proposed a battery algorithm to minimise the peak load demand. In [10], different rule-based strategies for battery systems were implemented to examine their efficiency in reducing peak demand. Overall, despite the unanimous consensus among these studies on the importance of reducing peak demand, they did not provide a cost-benefit analysis for their models from the viewpoints of different stakeholders. A cost-benefit study is essential because the CBS owner (whether an aggregator or a utility company) will not attempt to reduce the peak load unless it is economically sensible. For this reason, the authors in [11] proposed an online algorithm for battery systems that minimises both the energy usage charge and peak demand charge. However, they considered a fixed battery size and did not evaluate the trade-off between the maximum peak demand threshold and the battery capacity. In summary, this group of studies focused only on one aspect of the problem, i.e., ensuring a sufficient battery size or reducing the maximum peak demand threshold.

While battery sizing studies considering peak demand charge were developed in [12], [13], the authors assumed a perfect forecast for one month ahead, which is unrealistic given the high level of uncertainty for the long forecast horizon. In [14], the model considered a shorter horizon by constructing a daily operation framework to minimise the peak demand charge. Nonetheless, the results may not accurately reflect the true electricity cost since the peak demand charge is based on the maximum power consumption over a billing period, which typically spans one month or one year [2]. The prolonged billing period of the peak demand charge, together with the high investment cost on battery capacity, used to mitigate the charge, necessitates a thorough planning model when choosing an optimal CBS size.

In addition to using CBS for peak load shaving, several studies have focused on leveraging demand-side flexibility that comes as a feature of smart grid developments [15]. With the assistance of a home energy management system (HEMS), modern prosumers can shift their consumption to off-peak intervals by adjusting their demand based on electricity prices. To anticipate the reaction of prosumers in a highly dynamic electricity pricing environment, many price-responsive models for prosumers have been proposed [16]. In [17]–[19], the authors considered a nonlinear demand response program such that prosumers gain satisfaction for consuming electricity. However, consuming more electricity should not necessarily result in greater satisfaction depending on the time of day. In contrast, the works in [20], [21] considered discomfort for load curtailment, but treated each time interval separately. Since most of residential electricity usage comes from shiftable loads [22], it is crucial to consider the time-coupling effect of load rebound when constructing the price-responsive model. In [14], [23], the authors considered the discomfort caused by the load shifting. However, the effect of the load rebound effect was not considered. The work in [24] proposed a model for the rebound effect of shiftable loads, but the prosumers' discomfort was neglected. In [22], the authors considered both the discomfort and the effect of load shifting. Despite this, the program was designed for a predefined flat rate or time-of-use (ToU) tariff structure, and not suitable for modelling prosumers' consumption under the dynamic fluctuations of real-time (RT) wholesale market prices. Although all existing studies incorporated price-response parameters into their models, the coefficients lacked statistical significance and were arbitrarily selected to fit those studies.

B. Objectives and contributions

To accurately model prosumers' behaviour under a time-varying pricing scheme, this paper proposes a price-responsive model for prosumers' consumption considering their discomfort with load shifting. In contrast to the existing work focusing on a predefined flat rate or ToU tariff, this model is suitable for modelling prosumers' behaviour under the RT price fluctuations. In addition, it can be customised according to the characteristics of the individual prosumer and different times of the day using the concept of price elasticity. The CBS operator uses this model to anticipate the consumption curves of the local prosumers and optimise energy arbitrage and CBS discharging accordingly to minimise the energy usage charge and peak demand charge. To solve the aforementioned challenge of the prolonged billing period of peak demand charge and battery investment for long horizons, we consider a receding horizon operation (RHO) model for CBS, where only the dispatch decision in the first interval is binding, while the rest are to ensure that the operating model is not myopic [25]–[27]. The optimisation must then be solved consecutively for the next receding horizons. For this reason, it is not possible to obtain the optimal CBS capacity and peak demand threshold

in a single-shot optimisation. Instead, different feasible values must be examined in an iterative manner to obtain the optimal solution. Although considering RHO in a planning problem can increase the computational burden, the significant capital expenditure and the long duration of a battery project necessitate correct modelling within the sizing framework. In [22], an exhaustive search was done to find the optimal battery size. Since we are looking for the ideal trade-off between the CBS capacity and peak demand threshold, the coupling between the two variables can greatly increase the number of combinations, making the exhaustive search infeasible or very time consuming. An algorithm based on Benders decomposition was proposed in [27] to reduce the number of iterations required to reach the global optimal battery capacity. However, in addition to peak charge, the prosumers' behaviour and battery degradation were neglected during sizing. In contrast, our model leverages Benders decomposition to decompose the RHO model into the planning and operational stage by considering CBS capacity and peak demand threshold as complicating variables while addressing the aforementioned shortcomings. Moreover, in the operational stage, we solve a bilevel program to model the strategic behaviour between the CBS owner and local prosumers. The main contributions of this paper are summarised below:

- Offering a prosumer price-responsive model that considers RT price fluctuations, financial compensation for the discomfort caused by load shifting, and the rebound effect of shiftable loads.
- Proposing an RHO framework for cost-effectively sizing CBS and finding the optimal peak demand threshold in a local neighbourhood, where both the CBS owner and the local prosumers would financially benefit.

The rest of the paper is structured as follows. We outline the proposed local neighbourhood structure with CBS in section II and explain the key features of the model in section III, both conceptually and mathematically. Then, we propose the methods for solving the operational and planning problem in sections IV and V, respectively. The results of a comprehensive simulation study are reported and discussed in section VI. Finally, we conclude the paper in section VII.

II. Local neighbourhood structure with CBS

In this local neighbourhood, the CBS owner together with the local prosumers form a local electricity market, in which the CBS owner can be regarded as the local market operator. It is assumed that the local market operator will interact with the utility grid to balance local generation and demand mismatch. For instance, when participating in the Australian National Electricity Market (NEM), the local market operator pays RT wholesale prices to procure electricity from the grid as a 'Customer' [28]. Since the Australian NEM is a spot market in which the dispatch values are obtained for the next interval ahead, only the wholesale price in the first interval of the receding horizon must be binding, while prices in subsequent intervals can vary as time proceeds. Hence, it is necessary to consider RHO in the operation of the local market. Since price forecasting is outside the scope of this paper, we assume that the RT prices are perfectly known. In addition, we assume that the CBS operator cannot gain any financial benefit from exporting energy from the CBS to the power grid.

In this local market, the RT wholesale prices are passed on to local prosumers without any constraints on buying and selling. Therefore, prosumers can buy and sell electricity at the same RT prices. This is similar to that of Amber Electric, a newly founded electricity retailer in Australia [29]. We have also considered an export limit on rooftop PV systems, as introduced by most states in Australia, to maintain the integrity of the network and avoid over-voltages and congestion [30]. To make a profit, Amber Electric charges a monthly subscription fee of AUD$15 while prosumers purchase electricity at RT prices. In addition, prosumers are responsible for paying network charges, including the energy usage tariff and the peak demand tariff [2]. In their model, although prosumers can avoid energy usage charges by shifting their load to midday, they are still susceptible to a high electricity bill if they do not decrease their peak power consumption. In our model, however, the local market operator pays for the peak demand tariff for the local energy community and utilises the CBS system to manage and control the maximum peak load. In return, the local market operator will introduce mark-up (MU) prices on top of the RT prices, which can either be positive or negative depending on the local net load at every interval. For example, during periods of high demand, the operator may offer positive MU prices. In contrast, the MU prices may be negative when there is a reverse power flow from the community to the power grid. While introducing MU prices might indicate that local prosumers have to bear an additional cost when participating in the local market, we demonstrate that an overwhelming majority of prosumers pay less in a year due to the elimination of the peak demand tariff. The savings achieved from avoiding the peak demand charge can offset the added cost of MU prices, resulting in a lower overall cost for most prosumers. For those prosumers who experience increased electricity bills under this model, the local market operator offers compensation based on a Bill Guarantee scheme for expenses incurred [31]. Lastly, the local market operator can use the MU prices to activate prosumers' flexibility in a way that would decrease the peak demand. This helps to reduce prosumers' consumption during peak hours while allowing the operator to maintain a high profit. In this paper, we consider flexibility to be an aggregated flexibility of all loads. This consideration ensures that prosumers' privacy is respected, as it eliminates the need for the local market operator to dive into individual load details.

The structure of the local market operation can be summarised as follows. First, the operator forecasts the RT prices and the baseline net energy profiles in the local community for one day ahead. Then, the operator optimises the MU prices and passes the MU and RT prices, collectively referred to as 'local prices', to the local prosumers. Each prosumer then uniquely reacts to the price signals based on their price-responsive model, consisting of electricity payment and discomfort caused by load shifting. Lastly, given the adjusted consumption of the prosumers, the operator can optimally run the CBS to maximise profit. Since this paper considers the

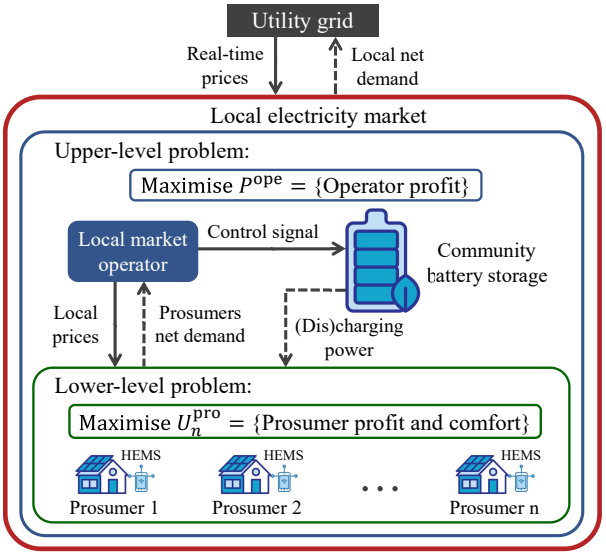

Fig. 1: Schematic diagram of the local electricity market

RHO approach, this process is repeated consecutively for the next receding horizon, where each receding horizon has a one-day lookahead. Taking into account the hierarchical nature of decision making and the separate objectives of the operator and the prosumers, the model is an instance of the Stackelberg game, in which the prosumers can be considered rational by administering a HEMS. The bilevel local market structure based on the Stackelberg game is shown in Fig. 1.

III. Problem Definition

In this section, we elaborate on the application of RHO when operating the local market and introduce the models for prosumers' price responsiveness and battery degradation.

A. Receding horizon operation (RHO)

We denote the set of local prosumers by $N = \{1, 2, \ldots, |N|\}$, where n is the index of prosumers. In RHO, instead of solving over the entire sizing horizon, i.e., $T = \{1, 2, \ldots, |T|\}$, the optimisation problem needs to be solved sequentially for each lookahead horizon, i.e., $H_j = \{j, j+1, \ldots, j+|H_j|-1\}$, where $H_j \subseteq T$. Therefore, we denote the first interval of each receding horizon, H_j, by $t = j$. Although it is possible that $H_j = T$, the work in [27] showed that a one-day lookahead would be sufficient to operate battery systems in distribution networks. Considering the daily patterns of rooftop PV systems and residential demand, and the inaccuracy in demand and PV generation forecast for longer periods, a one-day lookahead is chosen as the length of the receding horizon.

While the model assumes perfect forecasts, the dynamic nature of the RHO problem can cause the optimal value of the decision variables, such as prosumers' consumption and CBS (dis)charging power, at a specific time interval to vary from one receding horizon to another. Note that in each receding horizon H_j starting at j, we only commit the solutions in the first interval and then repeat the optimisation in $j+1$. Moreover, due to the inter-temporal constraints of the problem, some of the solutions from the previous horizons need to be considered in the subsequent horizons as initial state inputs. For example, the previous battery state-of-charge (SoC), battery capacity degradation and prosumers' realised demand are required in each new receding horizon. The previous battery information is required to calculate the battery SoC evolution through time in consecutive receding horizons. The previous prosumers' demand is used for the rebound effect constraints. In most studies that consider the rebound effect, e.g., [22], [32], the rebound could occur for as long as a day, which is unrealistic for most household appliances. Hence, in this paper, we consider a rebound horizon, H_j^{RB}, shorter than the receding horizon for which we solve the optimisation, where $H_j^{\mathrm{RB}} \subset H_j$.

B. Prosumers' price-responsive (utility) model

Prosumers' price-responsive (utility) functions concerning both the cost of electricity and prosumer (dis)comfort are widely adopted in the literature [16], [22]. While their models successfully capture the price responsiveness for each interval, they fail to represent the inter-temporal characteristic of shiftable loads. For example, consider a horizon with two intervals where $\lambda_{t=1}^{\mathrm{RT}} = \$0.5$/kWh and $\lambda_{t=2}^{\mathrm{RT}} = \$0.1$/kWh. Let's assume that $\lambda_{t=1}^{\mathrm{RT}}$ is reduced from \$0.5/kWh to \$0.3/kWh. Although existing studies would interpret this price reduction as the signal to increase the consumption of prosumers in $t = 1$, this is not in the best financial interest of prosumers as they can gain greater benefits if they can shift their load from $t = 1$ (reducing consumption) to $t = 2$, as long as $\lambda_{t=1}^{\mathrm{RT}} > \lambda_{t=2}^{\mathrm{RT}}$. Therefore, in this paper, the utility function in each time interval will look for one receding horizon ahead (i.e., one day ahead) and pick the lowest expected RT price, $\lambda_{\min,t}^{\mathrm{RT}} := \min\{\lambda_t^{\mathrm{RT}} | t \in H_j\}$ as a price reference when calculating the value of the utility function. We also consider the price elasticity concept for modelling prosumers' behaviour. As pointed out in many research studies, e.g., [33], [34], electricity is a commodity with relatively low price elasticity, $|\beta_{n,t}| < 1$, with the lowest price responsiveness after midnight. As a result, in our model, we consider different price elasticities based on the time period, with the highest price elasticity happening in peak hours and the lowest elasticity coefficient during off-peak hours. In addition, unlike the models in [17]–[19], we avoid the unrealistic assumption that prosumers will gain positive comfort by increasing their consumption. This restriction implies that the prosumers' decision to shift their load is purely driven by economic purposes, ensuring the effectiveness of the local price changes in modifying the prosumers' behaviour. Assume the utility function for prosumer n as:

$$\text{Utility} = \sum_{t \in H_j} \left[\lambda_t^{\mathrm{RT}}(G_{n,t} - x_{n,t}) + C(x_{n,t})\right], \tag{1a}$$

$$C(x_{n,t}) = \lambda_{\min,t}^{\mathrm{RT}} \left(1 + \frac{[x_{n,t} - \hat{x}_{n,t}]^-}{2\beta_{n,t}\hat{x}_{n,t}}\right) [x_{n,t} - \hat{x}_{n,t}]^-, \tag{1b}$$

where $x_{n,t}$ and $\hat{x}_{n,t}$ represent the prosumers' original expected consumption and the adjusted consumption after considering

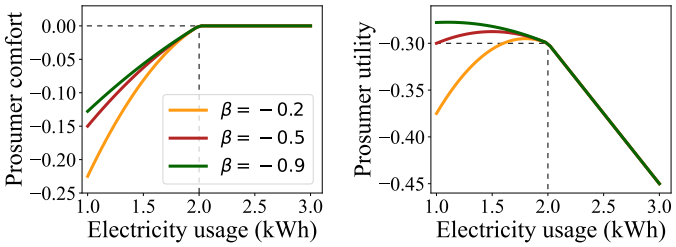

(a) Prosumers' comfort at different electricity usage value

(b) Prosumer utility when the RT price is \$0.15/kWh

Fig. 2: Prosumers' comfort and utility at different price elasticities

load shifting, respectively. The first term in (1a) represents the payment for net electricity generation, and the second term represents the prosumers' comfort as described by the quadratic function in (1b). It can be seen that the prosumers' comfort function depends on various factors, namely price reference, expected consumption and time-varying price elasticity coefficient. Note that the prosumers' comfort is the opposite of discomfort. The term $[x_{n,t}-\hat{x}_{n,t}]^-$ in (1b) denotes that the model only considers negative values from the subtraction due to the comfort restriction mentioned above. In this formulation, we aim to maximise the utility function with the highest payment for electricity export and prosumers' comfort. Fig. 2a shows prosumer comfort with varying price elasticity coefficients when $\hat{x}_{n,t} = 2$ kWh and $\lambda^{\text{RT}}_{\text{min},t} = \$0.1$/kWh. It can be seen that prosumers cannot gain any comfort by increasing consumption from their expected demand but will receive negative values in the comfort function for reducing their usage. Therefore, shifting loads to different intervals only decreases the prosumer's utility. Figure 2b depicts the utility of prosumers when $\lambda^{\text{RT}}_t = \$0.15$/kWh. Since this price is higher than the lowest expected price in the current receding horizon, $\lambda^{\text{RT}}_t > \lambda^{\text{RT}}_{\text{min},t}$, the prosumer may avoid consuming electricity in this interval and shift their loads to lower-price periods. Meanwhile, shifting the load to other intervals would increase the cost at those intervals. Furthermore, the decision to shift the load only applies to highly elastic prosumers in this case, as indicated by the green and red lines in Fig. 2b. This interplay between the multi-period electricity cost, the prosumer's discomfort and the rebound effect of shiftable load highlights the need for an effective pricing scheme to obtain the required flexibility. Hence, for the local prices, the operator will introduce MU prices on top of the RT prices to indirectly regulate prosumers' behaviour.

C. Battery degradation model

Since the CBS system is an essential component of the proposed business' economic viability, it is necessary to construct a comprehensive battery degradation model. This paper considers the cyclic and calendar battery degradation inspired by the experimental model in [35] as follows:

$$Q^{\text{cyc}}_t = \sum_{m=1}^{t} (a\mathcal{T}^2 + b\mathcal{T} + c) \cdot e^{(\kappa\mathcal{T}+\xi)\frac{P^{\text{dis}}_m}{E^{\text{cap}}}} \cdot \frac{P^{\text{dis}}_m}{E^{\text{cap}}} \Delta t, \tag{2a}$$

$$Q^{\text{cal}}_t = \eta \cdot t^{0.5} \cdot e^{\frac{E_a}{R\mathcal{T}}}. \tag{2b}$$

As seen in (2a), the cyclic degradation model is nonlinear due to the multiplication of the exponential function and the decision variables. However, since xe^x is convex for all $x > 0$, we may approximate it with a piece-wise linear (PWL) function [36]. While the coefficients in the model from [35] show that the battery will reach its end-of-life (EoL) after seven years if it operates at least one cycle per day at $\mathcal{T} = 20°\mathbf{C}$, we have scaled the coefficients in (2b) to make the CBS system last ten years before reaching EoL at 70% of the original capacity. This threshold is chosen based on the warranty term of many commercial batteries, e.g., Tesla Powerwall [37].

IV. Local Market Operation

In this section, we formulate the bilevel optimisation for the operation of the local market and propose a solution to solve the problem analytically.

A. Bilevel optimisation problem

The proposed Stackelberg game can be formulated as a bilevel program in which the leader is the local market operator responsible for setting the MU prices. The followers are the prosumers who can shift their loads. The optimisation model of the bilevel program for receding horizon j is as follows:

Upper Level Problem:

$$\max_{\mathbf{\Psi}^{\text{ope}}} P^{\text{ope}}_j = \sum_{t\in H_j}\sum_{n\in N} \left[(\lambda^{\text{RT}}_t + \lambda^{\text{MU}}_t)(x^+_{n,t} - x^-_{n,t})\right] - \lambda^{\text{peak}}\zeta$$
$$-\sum_{t\in H_j}(B^{\text{cyc}}_t + B^{\text{cal}}_t) - \sum_{t\in H_j}\lambda^{\text{RT}}_t n^+_t - \sum_{t\in H_j}\lambda^{\text{oNW}}_t P^{\text{ch}}_t \Delta t, \tag{3a}$$

s.t.

$$\underline{\lambda}^{\text{MU}} \le \lambda^{\text{MU}}_t \le \overline{\lambda}^{\text{MU}} \quad \forall t \in H_j, \tag{3b}$$

$$\sum_{n\in N}\left(x_{n,t} - G^u_{n,t}\right) + P_t\Delta t = n^+_t - n^-_t \quad \forall t \in H_j, \tag{3c}$$

$$n^+_t \le \zeta\Delta t \quad \forall t \in H_j, \tag{3d}$$

$$E_t = E^{\text{init}} - \frac{1}{\Gamma}\sum_{m=j}^{t} P^{\text{dis}}_m \Delta t + \sum_{m=j}^{t} P^{\text{ch}}_m \Delta t \quad \forall t \in H_j, \tag{3e}$$

$$P_t = P^{\text{ch}}_t - P^{\text{dis}}_t \quad \forall t \in H_j, \tag{3f}$$

$$-\frac{E^{\text{cap}}}{T^c} \le P_t \le \frac{E^{\text{cap}}}{T^c} \quad \forall t \in H_j, \tag{3g}$$

$$\underline{\text{SoC}}\, E^{\text{cap}}\,(1 - Q^{\text{cyc}}_t - Q^{\text{cal}}_t) \le E_t \quad \forall t \in H_j, \tag{3h}$$

$$\overline{\text{SoC}}\, E^{\text{cap}}\,(1 - Q^{\text{cyc}}_t - Q^{\text{cal}}_t) \ge E_t \quad \forall t \in H_j, \tag{3i}$$

$$B^{\text{cyc}}_t = \frac{E^{\text{cap}} E^{\text{price}}(Q^{\text{cyc}}_t - Q^{\text{cyc}}_{t-1})}{1 - \text{EoL}} \quad \forall t \in H_j, \tag{3j}$$

$$B_t^{\text{cal}} = \frac{E^{\text{cap}} E^{\text{price}} (Q_t^{\text{cal}} - Q_{t-1}^{\text{cal}})}{1 - \text{EoL}} \quad \forall t \in H_j, \tag{3k}$$

$$E_t, P_t^{\text{ch}}, P_t^{\text{dis}}, n_t^+, n_t^-, B_t^{\text{cyc}}, B_t^{\text{cal}}, Q_t^{\text{cyc}}, Q_t^{\text{cal}} \geq 0 \ \ \forall t \in H_j, \tag{3l}$$

$$E^{\text{cap}}, \zeta \geq 0, \tag{3m}$$

Lower Level Problem:

$$\max_{\mathbf{\Psi_n^{pro}}} U_{n,j}^{\text{pro}} = \sum_{t \in H_j} \big[(\lambda_t^{\text{RT}} + \lambda_t^{\text{MU}})(x_{n,t}^- - x_{n,t}^+) - \lambda_t^{\text{pNW}} x_{n,t}^+ + C(x_{n,t}) \big] \quad \forall n \in N, \tag{3n}$$

s.t.

$$\underline{x}_{n,t} \leq x_{n,t} \leq \overline{x}_{n,t} \quad \forall n \in N, \ \forall t \in H_j, \tag{3o}$$

$$\sum_{t \in H_j^{\text{RB}}} x_{n,t} = \sum_{t \in H_j^{\text{RB}}} \hat{x}_{n,t} + \Delta x_{n,j} \quad \forall n \in N, \tag{3p}$$

$$G_{n,t}^u + G_{n,t}^s = G_{n,t} \quad \forall n \in N, \ \forall t \in H_j, \tag{3q}$$

$$x_{n,t}^- \leq \text{ExpL} \cdot \Delta t \quad \forall n \in N, \ \forall t \in H_j, \tag{3r}$$

$$x_{n,t} - G_{n,t}^u = x_{n,t}^+ - x_{n,t}^- \quad \forall n \in N, \ \forall t \in H_j, \tag{3s}$$

$$x_{n,t}, x_{n,t}^+, x_{n,t}^-, G_{n,t}^u, G_{n,t}^s \geq 0 \quad \forall n \in N, \ \forall t \in H_j, \tag{3t}$$

where $\mathbf{\Psi_n^{pro}} = \{x_{n,t}, x_{n,t}^+, x_{n,t}^-, G_{n,t}^u, G_{n,t}^s\}$, $\mathbf{\Psi}^{\text{ope}} = \{\lambda_t^{\text{MU}}, E^{\text{cap}}, E_t, P_t, P_t^{\text{ch}}, P_t^{\text{dis}}, n_t^+, n_t^-, B_t^{\text{cyc}}, B_t^{\text{cal}}, Q_t^{\text{cyc}}, Q_t^{\text{cal}}, \zeta\} \cup \mathbf{\Psi_n^{pro}}$. The upper-level problem is formulated in (3a)–(3m). As seen in (3a), the objective function of the operator contains six terms, namely local market profit, peak demand charge for the whole neighbourhood, cost of battery operation through cyclic and calendar degradation, cost of procuring electricity from the utility grid and network usage charge for CBS charging. The first constraint in (3b) defines the limit for the MU prices set by the operator in each interval. Note that λ_t^{MU} can be positive or negative, indicating an increase or a decrease in RT prices, respectively. Constraints in (3c)–(3d) restrict the net demand of the local neighbourhood from exceeding the peak demand threshold. We define the CBS operation in (3e)–(3i).Note that due to the cost associated with P^{ch} in (3a), the optimisation will never find simultaneous battery charging and discharging an optimal solution [38]. Hence, the complementarity constraints for P^{ch} and P^{dis} are unnecessary. Due to the sequential operation of the RHO and the binding decision on the first interval, we set the battery's initial SoC in j to be the actual SoC of the previous receding horizon as follows:

$$E^{\text{init}} = E_{j-1}, \tag{4}$$

where the initial SoC of the sizing horizon (i.e., when $j = 1$) is fixed to 0. Constraints in (3h)–(3i) represent the boundaries of the CBS SoC such that the maximum capacity is reduced over time due to capacity degradation. Lastly, (3j) and (3k), respectively, calculate the cost of cyclic and calendar degradation in interval t with respect to the EoL of the battery.

In the lower-level problem in (3n)–(3t), the objective function is slightly modified from (1a) to include the MU prices, λ_t^{MU}. We also introduced the network usage charge when prosumers import electricity, as shown in the second term. Constraint (3o) denotes that prosumers can vary their consumption with respect to their available flexibility. However, the rebound effect of shiftable loads must be maintained within the rebound horizon, H_j^{RB}, as ensured in (3p), where $\Delta x_{n,j}$ depicts consumption deviation from the first interval of the sizing horizon, $j = 1$, up to receding horizon $j - 1$ as follow:

$$\Delta x_{n,j} = \sum_{m=1}^{j-1} \big(\hat{x}_{n,m} - x_{n,m} \big). \tag{5}$$

Constraint (3q) splits the solar generation into 'used' and 'spilt' energy due to the export limit enforced by (3r). Lastly, we represent the prosumer's net demand in (3s).

B. Casting the bilevel model into a single-level problem

Analytically, the bilevel problem can be converted into a single-level Mathematical Program with Equilibrium Constraint (MPEC) by applying the strong duality theorem [36]. Conversion to MPEC ensures that the solutions obtained are the Stackelberg equilibrium [39]. However, since the comfort function in (1b) is quadratic, a bilinear term will emerge in the model from the dual of the lower-level problem, making the problem intractable. To address the issue, we first linearise the nonlinear terms using PWL approximation. Then, we apply the strong duality theorem to convert the lower-level problem in (3n)–(3t) into a set of constraints for the upper-level problem. Interested readers can refer to Appendix A and Appendix B for the formulation of the PWL approximation and strong duality theorem on the lower-level problem, respectively.

V. Solution for optimal CBS capacity and peak demand threshold

As mentioned in subsection III-A, the RHO must be solved sequentially, restricting the ability to find the optimal CBS capacity and peak demand threshold in a single optimisation for the length of data. Thus, we need to examine different value combinations of CBS capacity and peak demand threshold iteratively, emphasising the importance of finding the optimal solutions in fewer iterations. Benders decomposition was proposed in [27] to increase the computational efficiency of the battery sizing problem by reducing the number of iterations required to reach the optimal battery capacity. However, implementing the decomposition technique requires linearity, which is not the case in our model due to the nonlinearity of the bilevel program. This is due to the multiplication of λ_t^{MU} and $(x_{n,t}^+ - x_{n,t}^-)$ in (3a) and (3n) although note that (3n) has been replaced with constraints derived from the strong duality theorem. A common method to resolve nonlinearity in the bilevel program is to transform the MPEC to a mixed-integer linear programming (MILP) problem by discretising one of the variables, i.e., discretising λ_t^{MU} in our model [36]. However, the introduction of binary variables once again restricts the use of Benders decomposition. In this paper, we

utilise McCormick envelopes to relax the bilinear terms during the planning stage [40]. Once the optimal planning variables for the two mentioned strategies are obtained, we re-run the local market model with the MILP reformulation to calculate the ground truth cost of the system.

A. McCormick envelopes

Using McCormick envelopes, we can replace the bilinear terms, $\lambda_t^{\text{MU}}(x_{n,t}^{+} - x_{n,t}^{-})$, in (3a) with two new variables $z_{n,t}^{+}$ and $z_{n,t}^{-}$ and eight new inequality constraints [40]. Specifically, each added variable is bounded below by two convex envelopes and bounded above by two concave envelopes of the bilinear terms. The resulting regions bounded by those envelopes are the convex hull of these two sets:

$$D_{n,t}^{+} = \{(x_{n,t}^{+}, \lambda_t^{\text{MU}}, z_{n,t}^{+}) \in \mathbb{R}^3 | \,(3\text{b}), 0 \le x_{n,t}^{+} \le \overline{x}_{n,t}, \\ z_{n,t}^{+} = \lambda_t^{\text{MU}} x_{n,t}^{+}\}, \tag{6a}$$

$$D_{n,t}^{-} = \{(x_{n,t}^{-}, \lambda_t^{\text{MU}}, z_{n,t}^{-}) \in \mathbb{R}^3 | \,(3\text{b}), 0 \le x_{n,t}^{-} \le \text{ExpL} \cdot \Delta t, \\ z_{n,t}^{-} = \lambda_t^{\text{MU}} x_{n,t}^{-}\}. \tag{6b}$$

Remark. Since McCormick envelopes are exact if any of the inequalities in (6) and (3b) are binding [41], the solutions for the local market operation during the planning stage (i.e., including the McCormick envelopes) often match the exact solutions obtained by the MILP model in the operational stage, which is executed to calculate the ground truth cost and ensure the accuracy of relaxation. Specifically, during the night with no solar energy, we can usually see that λ_t^{MU} increases to $\overline{\lambda}_t^{\text{MU}}$ to maximise the operator's profit.

B. Benders decomposition

Since the local market model is linear after the McCormick relaxation, we can implement Benders decomposition. In (3), the complicating variables are the battery capacity E^{cap} and the peak demand threshold ζ, which must be determined once for the whole sizing horizon. Therefore, we can divide the problem into a planning stage, where we determine the values for E^{cap} and ζ; and an operational stage, where we sequentially solve the RHO while keeping E^{cap} and ζ as constants. In this case, the planning stage is the Benders' master problem.

1) Master problem: For each iteration i, the master problem is formulated as follows:

$$\max_{E^{\text{cap}(i)}, \zeta^{(i)}, \alpha^{(i)}} \; B^{\text{mas}(i)} = \alpha^{(i)} - \lambda^{\text{peak}} \zeta^{(i)} - B_{t=T^e}^{\text{cal}(i)}, \tag{7a}$$

s.t.

$$\alpha^{(i)} \le \alpha^{\text{up}}, \tag{7b}$$

$$\alpha^{(i)} \le T^e \big[\, B_s^{(k)} + \Upsilon_s^{(k)} \big(E^{\text{cap}(i)} - E^{\text{cap}(k)}\big) \\ + \Theta_s^{(k)} \big(\zeta^{(i)} - \zeta^{(k)}\big)\big] \quad \forall k \in [2, i-1], \tag{7c}$$

where α represents the proxy of the sub-problem objective values. Since we only have the data for one year, we scale the sub-problems' results by T^e. The parameters $\Upsilon_s^{(k)}$ and $\Theta_s^{(k)}$ are calculated as the weighted sum of the dual variables associated with equality constraints for E^{cap} and ζ, respectively, in all receding horizon sub-problems. Similarly, $B_s^{(k)}$ illustrates the weighted sum of the sub-problems' objective values. Constraint (7b) introduces an upper bound for α for the first iteration (i.e., $i = 1$). For subsequent iterations, Benders cuts are generated via (7c).

2) Sequential sub-problems: The sub-problems represent the operational stage of the local market under RHO setting. Thus, the planning variables are fixed via equality constraints to obtain their associated dual variables. Note that instead of solving the sub-problems in parallel, we need to solve them sequentially due to the coupling nature of RHO [27].

Proposition 1. *For a given planning solution $(E^{cap(i)}, \zeta^{(i)})$ obtained from the master problem in iteration i, the peak demand threshold constraint in* (3d) *is not always guaranteed. That is, there exists t such that $n_t^{+} > \zeta \Delta t$.*

Proof. Since Eq. (3d) is not considered in the master problem, both of the planning variables $(E^{\text{cap}(i)}, \zeta^{(i)})$ might be zero in a certain iteration. Because $x_{n,t}$ cannot be reduced below $\underline{x}_{n,t}$, which can only take non-zero values, we will have $n_t^{+} > 0$. As a result, (3d) is violated. □

Due to Proposition 1 and the utilisation of Benders decomposition and McCormick envelopes, the local market model in (3), which represents one sub-problem, is modified as follows:

$$\max_{\mathbf{\Psi}^{\text{sub}}} \; B_j^{\text{sub}(i)} = \sum_{t \in H_j} \sum_{n \in N} \big[\lambda_t^{\text{RT}} (x_{n,t}^{+} - x_{n,t}^{-})\big] + z_{n,t}^{+} - z_{n,t}^{-} \\ - \sum_{t \in H_j} \big(B_t^{\text{cyc}} + \lambda_t^{\text{RT}} n_t^{+} + \lambda_t^{\text{oNW}} P_t^{\text{ch}} \Delta t + \lambda_t^{\text{sl}} n_t^{\text{sl}}\big), \tag{8a}$$

$$\text{s.t. } (3\text{b})\text{–}(3\text{c}), (3\text{e})\text{–}(3\text{j}), (3\text{l}), (6), \tag{8b}$$

$$\text{Strong duality theorem for } (3\text{n})\text{–}(3\text{t}), \tag{8c}$$

$$n_t^{+} - n_t^{\text{sl}} \le \zeta \Delta t \quad \forall t \in H_j, \tag{8d}$$

$$E^{\text{cap}} = E^{\text{cap}(i)} : \; \Upsilon_j^{(i)}, \tag{8e}$$

$$\zeta = \zeta^{(i)} : \; \Theta_j^{(i)}, \tag{8f}$$

where n^{sl} is the new 'slack' variable to prevent the sub-problem from being infeasible due to the peak demand constraint in (3d). Thus, we modify (3d) as in (8d) and introduce a penalty coefficient λ_t^{sl} in (8a). We also replace the bilinear terms in (8c) with $z_{n,t}^{+}$ and $z_{n,t}^{-}$.

We use Algorithm 1 to find the optimal planning variables using Benders decomposition. Although the RHO only implements the dispatch decision in the first interval, the objective value in (8a) and the dual variables in (8e) and (8f) are representatives of the whole receding horizon H_j. This means that before passing these parameters to the master problem, we need to assign weights to them as follows:

$$B_s^{(i)} = \sum_{j=1}^{|T|} \frac{B_j^{\text{sub}(i)}}{|H_j|}, \Upsilon_s^{(i)} = \sum_{j=1}^{|T|} \frac{\Upsilon_j^{(i)}}{|H_j|}, \Theta_s^{(i)} = \sum_{j=1}^{|T|} \frac{\Theta_j^{(i)}}{|H_j|}. \tag{9}$$

C. Operator's profit calculation

As previously mentioned, upon obtaining the optimal planning variables from Benders decomposition, we will re-run the local market model as a MILP problem and calculate the operator's profit considering only the first interval of each receding horizon as follows:

$$P^{\text{ope}} = \sum_{j=1}^{|T|} \sum_{n \in N} \left[(\lambda^{\text{RT}}_{t=j} + \lambda^{\text{MU}}_{t=j})(x^{+}_{n,t=j} - x^{-}_{n,t=j}) - B^{\text{com}}_{n} \right] - B^{\text{sup}} - \sum_{j=1}^{|T|} \left(\lambda^{\text{RT}}_{t=j} n^{+}_{t=j} + \lambda^{\text{oNW}}_{t=j} P^{\text{ch}}_{t=j} \right) - \lambda^{\text{peak}} \zeta - E^{\text{cap}} E^{\text{price}}, \quad (10)$$

where $t = j$ denotes the first interval of each receding horizon H_j, and B^{sup} depicts the fixed daily supply charge in [2]. The term $B^{\text{com}}_{n} \in \mathbb{R}_{+}$ represents the compensation costs of the prosumers due to the Bill Guarantee scheme mentioned in section II, in which the operator compensates a few prosumers that have an increased cost under this model. The compensation can be determined by the operator via a constraint as follows:

$$\sum_{j=1}^{|T|} \left[(\lambda^{\text{RT}}_{t=j} + \lambda^{\text{MU}}_{t=j})(x^{-}_{n,t=j} - x^{+}_{n,t=j}) \right] + B^{\text{com}}_{n} \geq \Lambda_n \quad \forall n \in N, \quad (11)$$

Remark. The operator can ensure Bill Guarantee for each prosumer by setting Λ_n equal to the expected bill of the prosumer from another electricity retailer. In this paper, we assume that prosumers can choose from a retailer that only passes RT prices to prosumers. However, they must pay for peak demand charges and a daily fixed charge, similar to the electricity plan offered by Amber Electric [29].

Algorithm 1: Benders decomposition algorithm

initialization: set $\alpha^{\text{up}} \rightarrow +\infty$; set $\epsilon > 0$; set $i = 1$; set $\text{UB}^{(i)} \rightarrow +\infty$; set $\text{LB}^{(i)} \rightarrow -\infty$;
repeat
  Solve master problem (7);
  $[E^{\text{cap}(i)}, \zeta^{(i)}, \alpha^{(i)}] = \arg\max B^{\text{mas}(i)}$;
  for $j = 1 : |T|$ **do**
    Solve sub-problem (8);
    $[E_{t=j}, P_{t=j}, x_{n,t=j}, \Upsilon^{(i)}_{j}, \Theta^{(i)}_{j}] = \arg\max B^{\text{sub}(i)}_{j}$;
    Calculate the coupling variables in (2), (4) and (5) and pass them to the next RHO;
  end
  Calculate $B^{(k)}_{s}, \Upsilon^{(k)}_{s}, \Theta^{(k)}_{s}$ using (9);
  $\text{UB}^{(i)} = \alpha^{(i)} - \lambda^{\text{peak}} \zeta^{(i)} - B^{\text{cal}(i)}_{t=T^e}$;
  $\text{LB}^{(i)} = B^{(i)}_{s} T^e - \lambda^{\text{peak}} \zeta^{(i)} - B^{\text{cal}(i)}_{t=T^e}$;
  $i = i + 1$;
until $|UB^{(i)} - LB^{(i)}| \leq \epsilon$;
output: $E^{\text{cap}*}, \zeta^{*}$

VI. Simulation study

In this section, we demonstrate the benefits of our proposed framework for all stakeholders (i.e., prosumers and the local market operator). We run the models on real-world data and compare the results with existing business models.

TABLE I: Price elasticity coefficient values

	Off-peak	Shoulder	Peak
Price elasticity	$[-0.15, -0.25]$	$[-0.4, -0.6]$	$[-0.85, -0.95]$

TABLE II: Battery data and simulation parameters

Battery data		Simulation inputs	
Γ	90%	Δt	0.5 hours
$\underline{\text{SoC}}$, $\overline{\text{SoC}}$	0%, 100%	$\underline{\lambda}^{\text{MU}}$, $\overline{\lambda}^{\text{MU}}$	$-10, 10$ ¢/kWh
EoL	70%	$\underline{x}_{n,t}$, $\overline{x}_{n,t}$	$0.5\hat{x}_{n,t}$, $1.5\hat{x}_{n,t}$
T^c	2 hours	ExpL	5 kW
T^e	10 years	$\lvert H_j \rvert$	48 (24 hours)
E^{price}	AUD$900/kWh	$\lvert H^{\text{RB}}_{j} \rvert$	12 (6 hours)

A. Simulation setup

1) Prosumers profile: From the Solar Home dataset [42], we randomly selected 125 prosumers (households) in NSW with half-hourly gross solar energy and electricity consumption in 2012. Since the average rooftop solar PV capacity has grown significantly in recent years [43], we scaled up the solar energy profiles of all prosumers four times uniformly. Although all prosumers in our dataset have rooftop solar PV systems, a recent report [44] shows that slightly more than 30% of Australian households are equipped with rooftop solar PV. Therefore, we removed solar energy from 84 (67%) prosumers to make a realistic case. The average rooftop solar PV capacity of the remaining prosumers is 7.65 kWp. We selected the first week of each season (28 days) for our simulation study to save computation time while considering seasonality and variability in prosumers' behaviour and PV generation. As noted in subsection III-B, the prosumers' price elasticity varies depending on the time of day. Therefore, we adopted three-time bands and randomly assigned the coefficient values to each prosumer using a uniform distribution. Table I shows the ranges for price elasticity for each prosumer, where the time window is specified by the DNSP in NSW [2].

2) Electricity prices and charges: Although the prosumers' profiles are from 2012, we chose NSW RT prices from June 2021 to July 2022 (commensurate to the month range of the prosumers' profile) for our study to represent current RT prices [28]. According to [2], network tariffs are defined differently for different customers in the distribution network. Specifically, we assume prosumers are subject to the tariff code EA116 while the operator is exposed to the tariff code EA380 in NSW [2].

3) Battery data and simulation parameters: In this study, we reference our battery cost from [45]. We summarised the battery and other simulation parameters in Table II. The optimisation problems are solved using Gurobi® 9.0 for Python on an Intel Core i7 at 2.00 GHz CPU with 8 threads.

B. Simulation results

1) Optimal CBS capacity and peak demand threshold: As mentioned in section II, applying the MU prices is necessary to motivate prosumers' behaviour change during critical

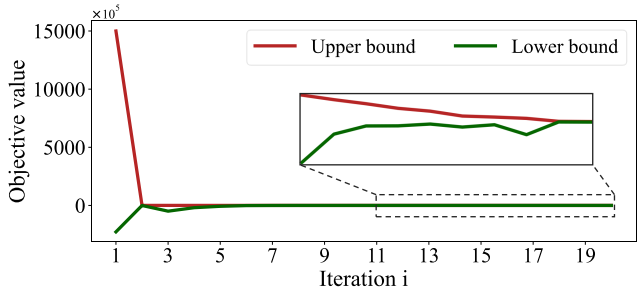

Fig. 3: Benders decomposition convergence rate for obtaining optimal CBS capacity and peak demand threshold

peak hours. Therefore, to demonstrate their effectiveness in reducing maximum peak demand, we run the optimisation with and without the MU prices. The scenario without MU prices represents the existing model, where only RT prices are passed on to local prosumers [29], [46]. Figure 3 demonstrates the convergence rate to obtain the optimal CBS capacity and peak demand threshold when considering MU prices. It can be seen that the algorithm requires 20 iterations to reach the ϵ-gap for the upper and lower bounds as specified in Algorithm 1. Each iteration takes approximately 1.5 hours to complete. Similarly, the algorithm takes the same number of iterations to converge for the case without MU prices. After obtaining the planning solutions from the Benders decomposition algorithm, we analyse the economic viability of the operator as discussed in subsection V-C. A summary of the results is given in Table III. The findings indicate that the peak demand threshold in our proposed local market model (**With MU**) is 9% lower than that of the existing methods (**W/o MU**) [29], [46]. Additionally, this result is achieved with a 41% smaller battery, highlighting the efficiency of implementing MU prices. The smaller battery also results in a shorter payback period (34% reduction), calculated based on (10). This is done using the optimal CBS capacity and the peak demand threshold obtained in the MILP problem in which λ_t^{MU} is discretised. To analyse the optimality of the solution obtained from the McCormick envelopes (**With MU**), we performed a local search around this solution. We found an optimal solution with a CBS capacity of 145 kWh and a peak demand threshold of 174 kW. The profit from this solution is just 1.9% higher than that achieved using the McCormick envelopes. However, it outperforms the **W/o MU** result by a significant 21%. Lastly, as mentioned in subsection III-C, we expect the CBS lifetime to be ten years if it cycles once per day. However, we observed that the CBS system could charge/discharge more than one cycle on some days. Despite this, we see that the expected lifetime is still close to ten years in both models.

TABLE III: Optimal planning variables and economic analysis

Models	Battery capacity	Peak threshold	Payback period	Expected lifetime
W/o MU	220 kWh	195 kW	5.3 years	9.8 years
With MU	130 kWh	177 kW	3.5 years	9.5 years

2) Local electricity profiles: Fig. 4 shows the local energy and pricing profiles of the MILP model with MU prices. The results are chosen from a weekday in January, which contains the highest peak demand in the given dataset. As shown in Fig. 4a, the local net demand is capped at the peak demand threshold, $\zeta = 177$ kW. This threshold is well below the original net demand of 286.5 kW, showing a decrease of 109.5 kW (38%). Furthermore, our proposed model results in an 85.6% reduction (289.7 kWh) in the cumulative reverse energy flow between hours 8:00 to 14:00. Note that we already consider the solar energy spilt in the original net demand due to the export limit, which was 138.7 kWh in total for the day. However, this aggregated spilt solar energy is reduced by 20.9 kWh (or 15%) in our local market optimisation model, as shown in Fig. 4b. This reduction can be attributed to the boost in self-consumption (resulting from load shifting) of local prosumers. In Fig. 4b, we can see that most of the exported electricity from prosumers is used to charge the CBS. Then, the CBS is used to keep the local net demand below the peak threshold by discharging from 20:00 to 23:00.

Regarding the electricity prices in Fig. 4c, we can see that the operator increases the local prices to the upper bound during the night to maximise its profit. However, with the excess solar generation during midday, the local prices are usually lower than the RT prices to encourage higher consumption by prosumers. Hence, the dynamic changes of local prices unlock higher flexibility of prosumers' consumption, leading to lower reverse power flow and peak demand in the network. As the MU prices increase to the upper bound, the results from McCormick envelopes become exact (optimal), as discussed in the Remark in subsection V-A. In particular, we observe that the constraints in (6) and (3b) are binding for approximately 78% of the simulation intervals. Additionally, the accuracy of McCormick envelopes is heavily influenced by the tightness of the feasible region [41], which is adequately constrained in (6) and (3b). For this reason, we expect that the values obtained in Table III closely approximate the globally optimal result.

3) Impact of load rebound: This can be observed in the variation of the MU prices in Fig. 4c. In particular, when solar energy decreases significantly at around 16:00, leading to positive net demand, local prices are still below RT prices to incentivise prosumers to increase their consumption and avoid consuming electricity during the evening peak demand hours. The MU price also plunges at 23:30 as a signal to prosumers to shift their load to this interval. The impact of the short rebound window is highlighted in Fig. 5, where we look at the expected and realised local consumption at 12:00 on the same day as in Fig. 4. Specifically, the figure shows the local consumption observed at five consecutive receding horizons prior to the realised consumption interval. It can be seen that the expected local consumption varies, even though the model considers perfect forecasts for the price and solar PV generation. This is because, while our approach considers one-day lookahead for each receding horizon, the rebound horizon is much shorter (it is a six-hour window). Consequently, in the receding horizons starting far before noon, such as 09:30 and 10:00, the prosumers' utility model finds that it is unnecessary to perform load shifting given the

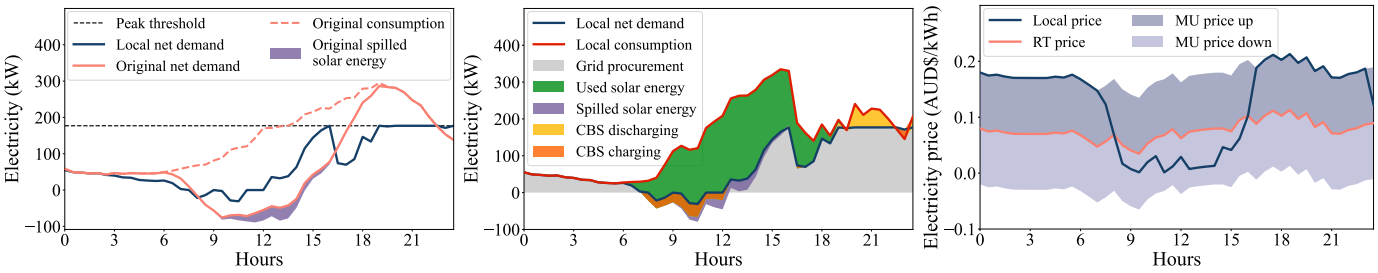

(a) Comparison of local net demand (b) Local market dispatch (c) Comparison of RT and local prices

Fig. 4: Local market operation of a weekday in January

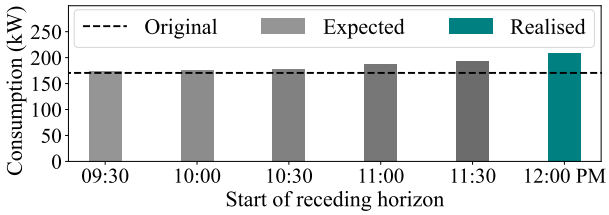

Fig. 5: Consumption at noon observed at the start of different receding horizons

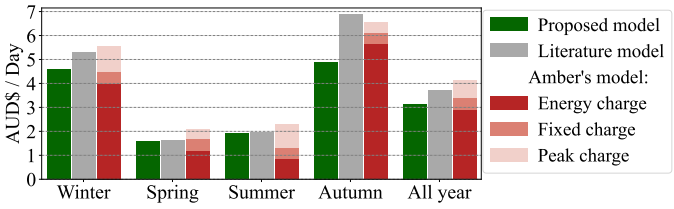

Fig. 6: Average electricity payment per prosumer per day

electricity prices in the next six hours. As a result, the expected consumption for noon remains unchanged from the original consumption. However, as the model approaches noon, it considers the generation and consumption forecasts for the late afternoon when electricity prices are expected to increase, i.e., higher RT prices and network usage charges. Therefore, expected consumption at noon increases to facilitate a decrease later in the afternoon. Consequently, the variations in expected consumption highlight the impact of quick load rebound and the need to update the expected CBS (dis)charging power at different receding horizons.

4) Prosumer electricity payment: Despite the high MU prices in many intervals, prosumers' electricity payment remains low because of the reduced spilt solar energy and the utilisation of demand-side flexibility. Fig. 6 shows the average electricity payment per prosumer per day in four seasons, where the green bars represent the payment using the proposed price-responsive model. To show the effectiveness of the proposed model, we compare it with two other models. The first model, referred to as the 'literature model', represents an existing price-responsive model in the literature, which inadequately captures prosumers' behaviour under the RT price fluctuations [16], [22]. To represent this model, we replace the $\lambda^{\text{RT}}_{\text{min},t}$ in (1b) with λ^{RT}_{t} and allow prosumers to 'gain' comfort for increasing consumption as in [17]–[19] by replacing $[x_{n,t}-\hat{x}_{n,t}]^-$ with $(x_{n,t}-\hat{x}_{n,t})$. The results for the literature model are represented by the grey bars. The second model is a business model similar to that of Amber Electric. The red stacked bars in Fig. 6 represent the payment when prosumers are not price responsive and only pay with RT prices. In addition, they have to pay for the peak demand charge referenced from the tariff code EA116 in [2], and a daily fixed charge of AUD$0.5/day, as referenced from Amber Electric [29]. In this study, we assumed a billing period of one year and already considered the Bill Guarantee mentioned in subsection V-C when calculating the annual average electricity payment in the proposed and literature models. Note that the reference for Bill Guarantee is by comparing with the payment each prosumer made under the business model of Amber Electric. If prosumers pay more under our proposed model or the literature model, we compensate them accordingly. In our proposed model, 14 prosumers (11%) required compensation. This indicates that those 14 prosumers had the same electricity bills as they would when participating in Amber's model, whereas the rest of the prosumers (111 prosumers) strictly paid less when participating in the local market with our proposed price-responsive model. Essentially, the losses incurred by those 14 prosumers come from the MU prices imposed on top of the RT prices. To ensure that all prosumers benefit positively from the proposed scheme, the local market operator can reduce the upper bound of the MU prices. This comes at the expense of a lower profit for the CBS owner. As a result, the best MU price cap will depend on the strategic priority of the local market operator: maximising profit through a higher MU price cap or attracting more prosumers by lowering this cap. However, setting it too low may hinder the effectiveness of MU prices in regulating prosumers' behaviour. Therefore, it is crucial to find a balance in determining the MU price cap and it stands as a strong candidate for future research. Under the chosen MU price cap, prosumers can decrease their annual electricity bills by 24% on average. Whereas, under the literature model, 39 prosumers (31%) were financially compensated by the local market operator, mainly due to the high payment in autumn. During this season, RT prices were the highest and prosumers under the literature model were less responsive to price fluctuations while also trying to gain comfort from increasing consumption. Overall, the proposed price-responsive model outperformed the existing models, demonstrating the effectiveness of local market participation and the importance of accurately characterising prosumers'

behaviour under the RT price fluctuations.

VII. Conclusion

In this paper, we proposed a price-responsive model for prosumers that adjusts their behaviour with respect to price fluctuations and the discomfort caused by load shifting while considering the time-constrained load rebound effect. Moreover, the formulation incorporates other practical features, including the residential export limit and network charges, to provide a realistic and comprehensive optimisation model. To reduce electricity bills for the local electricity community, we introduced a cost-effective framework for sizing and operating the CBS. The framework operates under the RHO regime and allows for efficient management and control of the maximum peak demand, ensuring that it remains below an optimal threshold and eliminating peak demand charges for local prosumers. Using the price-responsive model, the CBS owner, which also acts as a local market operator, can anticipate prosumers' behaviour and optimise the CBS (dis)charging power and the MU prices to maximise profit. The simulation results from real-world data of 125 prosumers show that both the CBS owner and the local prosumers can financially benefit from the proposed framework while also helping to reduce the peak demand of the local community. Future work could focus on adding local prosumers' stochastic behaviour and the provision of other services, such as ancillary services from CBS.

Appendix A
Piece-wise linear approximation of the comfort function

As mentioned in subsection IV-B, we want to solve the bilevel program analytically by applying the strong duality theorem to the lower-level problem. As such, we need to linearise the quadratic comfort function using piece-wise linear approximation. Since the comfort function $C(x_{n,t})$ is concave with respect to $x_{n,t}$ [47], we can reformulate the lower-level problem in (3n)–(3t) as follows:

$$\max_{\mathbf{\Psi_n^{pro}}} U_{n,j}^{\text{pro}} = \sum_{t\in H_j}\Bigg[(\lambda_t^{\text{RT}}+\lambda_t^{\text{MU}})(x_{n,t}^- - x_{n,t}^+) - \lambda_t^{\text{proN}} x_{n,t}^+ + C(\underline{x}_{n,t}) + \sum_{\omega\in W} S_{\omega,n,t}\, x_{\omega,n,t}\Bigg] \quad \forall n\in N, \tag{12a}$$

s.t.

$$x_{n,t} = \underline{x}_{n,t} + \sum_{\omega\in W} x_{\omega,n,t} :\ \gamma_{n,t} \quad \forall n\in N,\ \forall t\in H_j, \tag{12b}$$

$$x_{\omega,n,t} \le \frac{\overline{x}_{n,t}-\underline{x}_{n,t}}{||W||} :\ \mu_{\omega,n,t} \quad \forall \omega\in W,\ \forall n\in N,\ \forall t\in H_j, \tag{12c}$$

$$\sum_{t\in H_j^{\text{RB}}} x_{n,t} = \sum_{t\in H_j^{\text{RB}}} \hat{x}_{n,t} + \Delta x_{n,j} :\ \varphi_n \quad \forall n\in N, \tag{12d}$$

$$G_{n,t}^u + G_{n,t}^s = G_{n,t} :\ \theta_{n,t} \quad \forall n\in N,\ \forall t\in H_j, \tag{12e}$$

$$x_{n,t}^- \le \text{ExpL}\cdot\Delta t :\ \sigma_{n,t} \quad \forall n\in N,\ \forall t\in H_j, \tag{12f}$$

$$x_{n,t} - G_{n,t}^u = x_{n,t}^+ - x_{n,t}^- :\ \delta_{n,t} \quad \forall n\in N,\ \forall t\in H_j, \tag{12g}$$

$$x_{n,t}, x_{n,t}^+, x_{n,t}^-, G_{n,t}^u, G_{n,t}^s \ge 0 \quad \forall n\in N,\ \forall t\in H_j, \tag{12h}$$

$$x_{\omega,n,t} \ge 0 \quad \forall \omega\in W,\ \forall n\in N,\ \forall t\in H_j, \tag{12i}$$

where $\mathbf{\Psi_n^{pro}} = \{x_{n,t}, x_{n,t}^+, x_{n,t}^-, x_{\omega,n,t}, G_{n,t}^u, G_{n,t}^s\}$, $\omega \in W$ denotes the segments in the piece-wise linear model of the comfort function and $S_{\omega,n,t}$ depicts the slope of each piece-wise linear segment. We denote the dual variable for each primal constraint on the right-hand side of the colon.

Appendix B
Applying strong duality theorem on the lower-level problem

With the linear reformulation of the lower-level problem, we can apply the strong duality theorem to convert the lower-level problem into a set of constraints of the upper-level problem as follows:

$$\sum_{t\in H_j}\Bigg[(\lambda_t^{\text{RT}}+\lambda_t^{\text{MU}})(x_{n,t}^- - x_{n,t}^+) + \sum_{\omega\in W} S_{\omega,n,t}\, x_{\omega,n,t} - \lambda_t^{\text{proN}} x_{n,t}^+\Bigg] = \sum_{t\in H_j}\Bigg[\underline{x}_{n,t}\gamma_{n,t} + G_{n,t}\theta_{n,t} + \text{ExpL}\cdot\Delta t\,\sigma_{n,t} + \sum_{\omega\in W}\left(\frac{\overline{x}_{n,t}-\underline{x}_{n,t}}{||W||}\,\mu_{\omega,n,t}\right)\Bigg] + \left(\sum_{t\in H_j^{\text{RB}}}\hat{x}_{n,t} + \Delta x_n\right)\varphi_n \quad \forall n\in N, \tag{13a}$$

Constraints (12b)–(12i), (13b)

$$\gamma_{n,t} + \varphi_n + \delta_{n,t} \ge 0 :\ x_{n,t} \quad \forall n\in N,\ \forall t\in H_j^{\text{RB}}, \tag{13c}$$

$$\gamma_{n,t} + \delta_{n,t} \ge 0 :\ x_{n,t} \quad \forall n\in N,\ \forall t\in H_j\setminus H_j^{\text{RB}}, \tag{13d}$$

$$-\gamma_{n,t} + \mu_{\omega,n,t} \ge S_{\omega,n,t} :\ x_{\omega,n,t} \quad \forall \omega\in W,\ \forall n\in N,\ \forall t\in H_j, \tag{13e}$$

$$-\delta_{n,t} \ge -\lambda_t^{\text{RT}} - \lambda_t^{\text{proN}} :\ x_{n,t}^+ \quad \forall n\in N,\ \forall t\in H_j, \tag{13f}$$

$$\delta_{n,t} + \sigma_{n,t} \ge \lambda_t^{\text{RT}} :\ x_{n,t}^- \quad \forall n\in N,\ \forall t\in H_j, \tag{13g}$$

$$\theta_{n,t} - \delta_{n,t} \ge 0 :\ G_{n,t}^u \quad \forall n\in N,\ \forall t\in H_j, \tag{13h}$$

$$\theta_{n,t} \ge 0 :\ G_{n,t}^s \quad \forall n\in N,\ \forall t\in H_j, \tag{13i}$$

$$\sigma_{n,t} \ge 0 \quad \forall n\in N,\ \forall t\in H_j, \tag{13j}$$

$$\mu_{\omega,n,t} \ge 0 \quad \forall \omega\in W,\ \forall n\in N,\ \forall t\in H_j, \tag{13k}$$

where the constraint in (13a) represents the zero optimal duality gap between the primal and dual objective functions [48], while constraints in (13c)–(13k) represent the dual constraints for each primal variable.

ACKNOWLEDGMENT

This project is funded jointly by the University of Adelaide industry-PhD grant scheme and Watts A/S, Denmark. During the preparation of this work the authors used ChatGPT in order to improve readability and language. After using this tool, the authors reviewed and edited the content as needed and take full responsibility for the content of the publication.

REFERENCES

[1] Ausgrid. (2022) Ausgrid sub-threshold tariffs 2022-23. [Online]. Available: https://www.aer.gov.au/system/files/Ausgrid%20-%20Tariff%20trial%20notification%20-%202022-23_0.pdf

[2] ——. (2022) Es7 - network price guide. [Online]. Available: https://www.ausgrid.com.au/Industry/Regulation/Network-prices

[3] AER. (2023) Annual generation capacity and peak demand - nem. [Online]. Available: https://www.aer.gov.au/wholesale-markets/wholesale-statistics/annual-generation-capacity-and-peak-demand-nem

[4] Ausgrid. (2019) Demand tariff q & a. [Online]. Available: https://www.ausgrid.com.au/-/media/Documents/energy-use/tariffs/Demand-tariff-Q--A-for-residential-customers

[5] T. Conversation. (2022) 4 ways to stop australia's surge in rooftop solar from destabilising electricity prices. [Online]. Available: https://theconversation.com/4-ways-to-stop-australias-surge-in-rooftop-solar-from-destabilising-electricity-prices-173592

[6] Synergy. (2021) Alkimos beach energy storage trial final report. [Online]. Available: https://arena.gov.au/knowledge-bank/alkimos-beach-energy-storage-trial-final-report/

[7] J. Mair, K. Suomalainen, D. M. Eyers, and M. W. Jack, "Sizing domestic batteries for load smoothing and peak shaving based on real-world demand data," *Energy and Buildings*, vol. 247, p. 111109, 2021. [Online]. Available: sciencedirect.com/science/article/pii/S0378778821003935

[8] J. Li, "Optimal sizing of grid-connected photovoltaic battery systems for residential houses in australia," *Renewable Energy*, vol. 136, pp. 1245–1254, 2019. [Online]. Available: sciencedirect.com/science/article/pii/S096014811831173X

[9] Y. Mo, Q. Lin, M. Chen, and S.-Z. J. Qin, "Optimal online algorithms for peak-demand reduction maximization with energy storage," in *Proceedings of the Twelfth ACM International Conference on Future Energy Systems*, ser. e-Energy '21. New York, NY, USA: Association for Computing Machinery, 2021, p. 73–83. [Online]. Available: https://doi.org/10.1145/3447555.3464857

[10] M. B. Roberts, A. Bruce, and I. MacGill, "Impact of shared battery energy storage systems on photovoltaic self-consumption and electricity bills in apartment buildings," *Applied Energy*, vol. 245, pp. 78–95, 2019. [Online]. Available: https://www.sciencedirect.com/science/article/pii/S0306261919306269

[11] J. Shi, Z. Ye, H. O. Gao, and N. Yu, "Lyapunov optimization in online battery energy storage system control for commercial buildings," *IEEE Transactions on Smart Grid*, vol. 14, no. 1, pp. 328–340, 2023.

[12] H. S. Zhou, R. Passey, A. Bruce, and A. B. Sproul, "Aggregated impact of coordinated commercial-scale battery energy storage systems on network peak demand, and financial outcomes," *Renewable and Sustainable Energy Reviews*, vol. 144, p. 111014, 2021. [Online]. Available: https://www.sciencedirect.com/science/article/pii/S136403212100304X

[13] Z. Zhang, J. Shi, Y. Gao, and N. Yu, "Degradation-aware valuation and sizing of behind-the-meter battery energy storage systems for commercial customers," in *2019 IEEE PES GTD Grand International Conference and Exposition Asia (GTD Asia)*, 2019, pp. 895–900.

[14] Q. Yang, H. Wang, X. Wu, T. Wang, and S. Zhang, "Blockchain for transactive energy management of distributed energy resources in smart grid," in *Proceedings of the Twelfth ACM International Conference on Future Energy Systems*, ser. e-Energy '21. New York, NY, USA: Association for Computing Machinery, 2021, p. 211–215. [Online]. Available: https://doi.org/10.1145/3447555.3464848

[15] C. P. Mediwaththe, M. Shaw, S. Halgamuge, D. B. Smith, and P. Scott, "An incentive-compatible energy trading framework for neighborhood area networks with shared energy storage," *IEEE Transactions on Sustainable Energy*, vol. 11, no. 1, pp. 467–476, 2020.

[16] H. Aalami, M. Parsa Moghaddam, and G. Yousefi, "Evaluation of nonlinear models for time-based rates demand response programs," *International Journal of Electrical Power & Energy Systems*, vol. 65, pp. 282–290, 2015. [Online]. Available: sciencedirect.com/science/article/pii/S0142061514006243

[17] X. Jiang, C. Sun, L. Cao, L. Ngai-Fong, and K. H. Loo, "Peer-to-peer energy trading with energy path conflict management in energy local area network," *IEEE Transactions on Smart Grid*, vol. 13, no. 3, pp. 2269–2278, 2022.

[18] K. Anoh, S. Maharjan, A. Ikpehai, Y. Zhang, and B. Adebisi, "Energy peer-to-peer trading in virtual microgrids in smart grids: A game-theoretic approach," *IEEE Transactions on Smart Grid*, vol. 11, no. 2, pp. 1264–1275, 2020.

[19] Y. Jiang, K. Zhou, X. Lu, and S. Yang, "Electricity trading pricing among prosumers with game theory-based model in energy blockchain environment," *Applied Energy*, vol. 271, p. 115239, 2020. [Online]. Available: https://www.sciencedirect.com/science/article/pii/S0306261920307510

[20] M. Yu and S. H. Hong, "Incentive-based demand response considering hierarchical electricity market: A stackelberg game approach," *Applied Energy*, vol. 203, pp. 267–279, 2017. [Online]. Available: https://www.sciencedirect.com/science/article/pii/S0306261917307602

[21] M. Yu, J. Jiang, X. Ye, X. Zhang, C. Lee, and S. H. Hong, "Demand response flexibility potential trading in smart grids: A multileader multifollower stackelberg game approach," *IEEE Transactions on Systems, Man, and Cybernetics: Systems*, pp. 1–12, 2022.

[22] N. T. Dinh, S. A. Pourmousavi, S. Karimi-Arpanahi, Y. P. S. Kumar, M. Guo, D. Abbott, and J. A. R. Liisberg, "Optimal sizing and scheduling of community battery storage within a local market," in *Proceedings of the Thirteenth ACM International Conference on Future Energy Systems*, ser. e-Energy '22. New York, NY, USA: Association for Computing Machinery, 2022, p. 34–46.

[23] N. Liu, X. Yu, C. Wang, C. Li, L. Ma, and J. Lei, "Energy-sharing model with price-based demand response for microgrids of peer-to-peer prosumers," *IEEE Transactions on Power Systems*, vol. 32, no. 5, pp. 3569–3583, 2017.

[24] L. Werner, A. Wierman, and S. H. Low, "Pricing flexibility of shiftable demand in electricity markets," in *Proceedings of the Twelfth ACM International Conference on Future Energy Systems*, ser. e-Energy '21. New York, NY, USA: Association for Computing Machinery, 2021, p. 1–14. [Online]. Available: https://doi.org/10.1145/3447555.3464847

[25] K. Baker, G. Hug, and X. Li, "Energy storage sizing taking into account forecast uncertainties and receding horizon operation," *IEEE Transactions on Sustainable Energy*, vol. 8, no. 1, pp. 331–340, 2017.

[26] N. Christianson, L. Werner, A. Wierman, and S. Low, "Dispatch-aware planning for feasible power system operation," *Electric Power Systems Research*, vol. 212, p. 108597, 2022.

[27] P. Fortenbacher, A. Ulbig, and G. Andersson, "Optimal placement and sizing of distributed battery storage in low voltage grids using receding horizon control strategies," *IEEE Transactions on Power Systems*, vol. 33, no. 3, pp. 2383–2394, 2018.

[28] AEMO. (2022) Aemo. [Online]. Available: https://aemo.com.au/

[29] A. Electric. (2022) Amber electric. [Online]. Available: https://www.amber.com.au/

[30] S. P. Networks. (2021, apr) Upcoming changes to small embedded generation connections. [Online]. Available: https://www.sapowernetworks.com.au/data/310548/upcoming-changes-to-small-embedded-generation-connections/

[31] A. Electric. (2023) How is the bill guarantee calculated with the victorian government minimum feed-in-tariff? [Online]. Available: https://help.amber.com.au/hc/en-us/articles/360059804131

[32] G. De Zotti, S. A. Pourmousavi, J. M. Morales, H. Madsen, and N. K. Poulsen, "Consumers' flexibility estimation at the tso level for balancing services," *IEEE Transactions on Power Systems*, vol. 34, no. 3, pp. 1918–1930, 2019.

[33] Z. Csereklyei, "Price and income elasticities of residential and industrial electricity demand in the european union," *Energy Policy*, vol. 137, p. 111079, 2020.

[34] A. Knaut and S. Paulus, "Hourly price elasticity pattern of electricity demand in the german day-ahead market," EWI Working Paper 16/07, 2016. [Online]. Available: http://hdl.handle.net/10419/144865

[35] J. Wang, J. Purewal, P. Liu, J. Hicks-Garner, S. Soukazian, E. Sherman, A. Sorenson, L. Vu, H. Tataria, and M. W. Verbrugge, "Degradation of lithium ion batteries employing graphite negatives and nickel–cobalt–manganese oxide+spinel manganese oxide positives: Part 1, aging mechanisms and life estimation," *Journal of Power Sources*, vol. 269, pp. 937–948, 2014.

[36] S. Karimi-Arpanahi, M. Jooshaki, S. A. Pourmousavi, and M. Lehtonen, "Leveraging the flexibility of electric vehicle parking lots in distribution networks with high renewable penetration," *International Journal of Electrical Power & Energy Systems*, vol. 142, p. 108366, 2022.

[37] Tesla. (2022) Tesla powerwall. [Online]. Available: https://www.tesla.com/en_au/powerwall

[38] Z. Li, Q. Guo, H. Sun, and J. Wang, "Sufficient conditions for exact relaxation of complementarity constraints for storage-concerned economic dispatch," *IEEE Transactions on Power Systems*, vol. 31, no. 2, pp. 1653–1654, 2016.

[39] M. Zugno, J. M. Morales, P. Pinson, and H. Madsen, "A bilevel model for electricity retailers' participation in a demand response market environment," *Energy Economics*, vol. 36, pp. 182–197, 2013. [Online]. Available: https://www.sciencedirect.com/science/article/pii/S0140988312003477

[40] G. P. McCormick, "Computability of global solutions to factorable nonconvex programs: Part i — convex underestimating problems," *Mathematical Programming*, vol. 10, no. 1, pp. 147–175, Dec 1976.

[41] N. V. S. Mohit Tawarmalani, *Convexification and Global Optimization in Continuous and Mixed-Integer Nonlinear Programming*. Springer New York, NY, 2002.

[42] Ausgrid. (2012) Solar home electricity data. [Online]. Available: https://www.ausgrid.com.au/Industry/Our-Research/Data-to-share/Solar-home-electricity-data

[43] A. E. Council, "Solar report quarter 3, 2021," Tech. Rep., 2021. [Online]. Available: https://www.energycouncil.com.au/media/5zylveyr/australian-energy-council-solar-report_q3-2021.pdf

[44] ARENA. (2022) Solar energy. [Online]. Available: https://arena.gov.au/renewable-energy/solar/

[45] CSIRO, "Gencost 2021-22," Tech. Rep., 2022. [Online]. Available: https://www.csiro.au/-/media/News-releases/2022/GenCost-2022/GenCost2021-22Final_20220708.pdf

[46] J. Iria, P. Scott, A. Attarha, D. Gordon, and E. Franklin, "Mv-lv network-secure bidding optimisation of an aggregator of prosumers in real-time energy and reserve markets," *Energy*, vol. 242, p. 122962, 2022.

[47] F. C. Schweppe, M. C. Caramanis, R. D. Tabors, and R. E. Bohn, *Spot pricing of electricity*. Springer Science & Business Media, 2013.

[48] S. Boyd, S. P. Boyd, and L. Vandenberghe, *Convex optimization*. Cambridge university press, 2004.

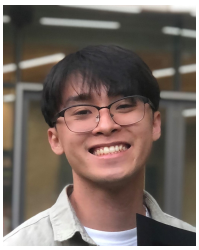

Nam Trong Dinh received his BSc (Honours) degree in Electrical and Electronic Engineering from the University of Adelaide, Adelaide, Australia in 2021. He is currently a PhD candidate in the School of Electrical and Mechanical Engineering at the same institution, where he is supported by a joint scholarship funded in collaboration with Watts A/S, Denmark. His research interests include demand response, business models for electricity retailers and aggregators, and battery energy management systems.

Sahand Karimi-Arpanahi received the BSc and MSc degrees in Electrical Engineering from the Sharif University of Technology, Tehran, Iran, in 2016 and 2018, respectively. He worked as a research assistant at Sharif University of Technology from 2018 to 2020. Since 2022, he has been with the Australian Energy Market Operator (AEMO). Also, he is currently a PhD candidate in the School of Electrical and Mechanical Engineering at the University of Adelaide, Adelaide, Australia, and CSIRO Energy, Newcastle, Australia. His research interests include power system optimisation; data analysis in power systems and electricity markets; and grid integration of renewable energy and battery storage systems.

S. Ali Pourmousavi (Senior Member, IEEE) received the B.Sc., M.Sc., and Ph.D. degrees (with hons.) in electrical engineering, in 2005, 2008, and 2014, respectively. From 2014 to 2019, he was with California ISO, NEC Laboratories America Inc., Technical University of Denmark, Kongens Lyngby, Denmark, and The University of Queensland, Brisbane, Australia. He is currently a Senior Lecturer in the school of Electrical and Mechanical Engineering, the University of Adelaide, Australia. His current research interests include mining and transportation electrification, BTM flexibility aggregation and demand response.

Mingyu Guo is a Lecturer in the Optimisation and Logistics group at the University of Adelaide. He received his Ph.D. degree in Computer Science from Duke University, USA. Prior to joining the University of Adelaide, he was a Lecturer in the Economics and Computation group at University of Liverpool, UK. His main research focus is algorithmic game theory and its applications, as well as combinatorial optimisation via neural networks and evolutionary computation.

Jon A. R. Liisberg received the B.Sc. degree in Mathematics from University of Copenhagen, Denmark in 2013. He received the M.Sc. and Ph.D. degrees in Mathematical modeling and computation from Technical University of Denmark in 2015 and 2019. The Ph.D. was jointly funded by Innovation Fund Denmark and Watts A/S. He is currently employed as a Data Scientist by Watts A/S, with focus on analysis and modeling of residential utility consumption.